This manuscript was published as formal in:

International Journal of Biological Macromolecules 2020, 162, 1323-1337

DOI: 10.1016/j.ijbiomac.2020.06.218

https://doi.org/10.1016/j.ijbiomac.2020.06.218

***Title*:**

Citryl-imine-PEG-ylated chitosan hydrogels – promising materials for drug delivery applications

Daniela Ailincai[1], Liliana Mititelu-Tartau[2], Luminita Marin[1]

[1]"Petru Poni" Institute of Macromolecular Chemistry, Grigore Ghica Voda Alley, Iasi, Romania

[2]"Grigore T. Popa" University of Medicine and Pharmacy, Iasi, Romania

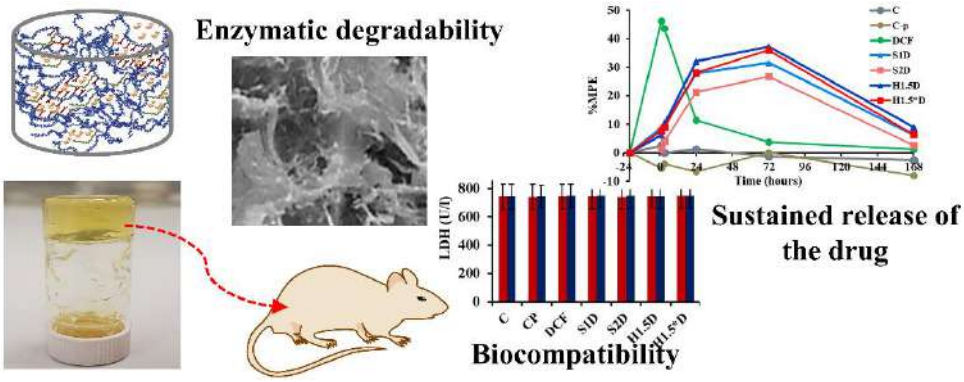

Abstract

The present paper focuses on the synthesis and characterization of new hydrogels and drug delivery systems, designed for local therapy. The hydrogels were obtained by reacting PEG-ylated chitosan derivatives with citral in different molar ratios of their functionalities. The drug delivery systems were obtained by the *in situ* hydrogelation of PEG-ylated chitosan derivatives with citral, in the presence of a hydrophilic anti-inflammatory drug, diclofenac sodium salt. The hydrogels and the drug delivery systems were characterized from the structural, supramolecular and morphological points of view by FTIR spectroscopy, wide angle X-ray diffraction, polarized optical microscopy and scanning electron microscopy. The *in vitro* release kinetics of the drug has been monitored in physiological conditions, while the *in vivo* release was evaluated by the somatic pain model on rats. The *in vitro* enzymatic degradability of the hydrogels was evaluated in the presence of lysozyme, leading to a significant mass loss of 47 % in 21 days. All the findings, recommend the investigated materials as promising candidates for local drug delivery applications.

Keywords: PEG-ylation, chitosan hydrogels, local drug delivery, sustained drug release, antinociceptive effect, biocompatibility

1. Introduction

Local drug delivery is a central field of biomedicine related research, whose development promises breakthrough advances to human health [1,2]. Comprising a large variety of systems and formulations, local drug delivery aims to transport pharmaceutical active compounds at the desired site of action, creating the framework for its maximum therapeutic effect, increasing its bioavailability and decreasing its side effects in the rest of the body [3,4]. The existence of plenty of drugs and drugs matrix, makes the field of drug delivery and local drug delivery, a complex one in which continuous development and innovation are required [5-7].

Among the large variety of drug delivery systems used in local therapy, hydrogels are known as the superlative one, due to their physical peculiarities: porosity, similarity to tissues due to their high-water content, biocompatibility, safety, ability to swell or shrink under certain conditions and so on [8-10]. Beside the advantages mentioned above, the hydrogels based on chitosan, have the plus of chitosan's intrinsic therapeutic properties, and maybe more important, their compositional and mechanical similarity to the extracellular matrix [11]. This is the reason why, in the last years, plenty of studies developed and investigated biomaterials based on a large variety of chitosan derivatives, such as chitosan-grafted-dihydrocaffeic acid [12- 1], N-

carboxyethyl chitosan [13, 14 – 2, 7], carboxymethyl chitosan [15 - 4], quaternized chitosan [16 - 6] or chitosan-graft-polyaniline [17- 3]. All these materials proved outstanding properties, showing once more the high potential of chitosan to generate valuable biomaterials. Moreover, due to the presence of the amino groups on chitosan backbone, this polymer represents a workbench for the development of dynamic hydrogels, based on reversible imine linkages [18, 19]. By this, the structural and mechanical defects in the resulted hydrogels are minimized, leading to materials which may respond uniformly in terms of oxygen permeability and drugs diffusivity [20].

A large variety of hydrogels based on chitosan have been reported in the literature, obtained by its physical or chemical crosslinking, the last one being achieved usually with dialdehydes. Moreover, in the last years, in our group, was developed a new strategy of crosslinking chitosan with biologically friendly monoaldehydes [21-26].

Among the hydrogels synthesized by us, the one based on chitosan and citral proved excellent *in vivo* biocompatibility and thixotropic behavior, important characteristics for their future bio-applications [26]. However, due to the fact that the crosslinking nodes of these materials were highly hydrophobic clusters formed by hydrophobic-hydrophobic associations, they presented poor ability to rehydrate after lyophilization. This aspect clearly limited its potential of being used in cell growing or drug delivery applications.

With this in mind, we proposed the use of PEG-*g*-chitosan as precursors for the obtaining of citryl-imine-chitosan hydrogels with improved properties. Poly(ethylene glycol), is one of the few synthetic polymers which was approved by the FDA for being used in food, cosmetics and pharmaceutical industry. In bio-related applications, the presence of PEG in formulations or systems proved to bring important advantages, such as increased biocompatibility, prolonged blood circulation and stealth behavior [27]. The chitosan PEG-ylation was already used as a method to improve chitosan's physicochemical and biological properties or even to add new ones [28]. Moreover, PEG-ylated chitosan derivatives promoted the obtaining of thermosensitive or bioadhesive hydrogels which were successfully used as drugs or proteins delivery systems, even if the used crosslinkers were not completely biologically friendly *e.g. glutaraldehyde* [29-31]. Therefore, we decided to synthesize PEG-ylated chitosan derivatives by the acid condensation of chitosan with PEG-monoaldehyde in two molar ratios of their functionalities. In this manner, two imino-PEG-ylated chitosan derivatives with different hydrophilicity were formed. Due to the fact that the imine linkage is known to be reversible in the presence of water molecules, the imino-PEG-ylated chitosan derivatives should present dynamicity. If proved to be so, they will be subjected to reductive amination, leading to amino-PEG-ylated chitosan derivatives which will be used as precursors

for hydrogels and drug delivery systems obtaining by the reaction with citral, a biologically friendly monoaldehyde. We considered that this approach will lead to materials with increased hydrophilicity and improved properties in general, closer to the standards imposed for bio-applications.

2. Rational design

The hydrogels design was thought out in order to fulfill the requirements for use as matrix for drug release systems, such as biocompatibility, biodegradability, lack of toxicity and proper swelling, which are mandatory for bioapplications. To this aim, the chitosan, well known for its biodegradability, biocompatibility and lack of toxicity was firstly combined with PEG to improve its hydrophilicity in physiological medium. Further, the hydrogelation was realized with citral, a naturally originating aldehyde, which already proved ability to crosslink chitosan by a supramolecular aggregation mechanism [26, 32]. Citral was chosen as an alternative to traditional dialdehyde crosslinkers which over time proved a degree of toxicity limiting the bioapplications [vezi referintele]. It is a biocompatible monoaldehyde extracted from lemon essential oil, with a LD> 1000 mg / Kg body, which is rapidly metabolized and excreted [33]. It should be stressed that PEG is a synthetic polymer approved by the FDA in order to be used in food and pharmaceutical industry, being already demonstrated its capacity to improve the biocompatibility, the blood circulation time and stealth behavior, when used in biomaterials [27].

2. Materials and methods

2.1 Materials

Citral (95%), chitosan (217.74 kDa, DA: 85%), O-[2-(6-Oxocaproylamino)ethyl]-O′-methylpolyethylene glycol 2000, phosphate buffer (pH= 7.4), diclofenac sodium salt (DCF), lysozyme (lyophilized powder, protein 90%, 40000 units/mg protein) and ethanol were purchased from Aldrich and used without any previous treatments.

2.2 The synthesis of the imino- PEG-ylated chitosan derivatives (**D** samples) was done by chitosan imination with PEG-aldehyde in two molar ratios of their functionalities 40 to 1 (**D1**) and 50 to 1 (**D2**) (Scheme 1). The certain amounts of reagents are given in Table S1.

2.3 The synthesis of the amino- PEG- ylated chitosan derivatives (**S** samples) has been done by the reductive amination in heterogeneous system with sodium borohydride in excess (10:1 molar ratio) of the D1 and D2 imines to give S1 and S2 amine derivatives (Scheme S1), according to a procedure described in the literature [34].

2.4 Synthesis of the hydrogels (**H1-H2.5 and H1*-H2.5*** samples)

A series of 8 hydrogels was obtained *via* the acid condensation reaction of the free amino groups of **S1** and **S2** derivatives with the aldehyde group of citral, in different molar ratios of their functionalities (**H** series based on **S1** derivative and **H*** series based on **S2** derivative), according to an experimental procedure previously developed in our group [21-26] (Scheme 1, Table S2). A reference sample, based on citryl-imine-chitosan (CC2) was also synthesized according to a previously described protocol [26].

2.5 *Synthesis of the drug delivery systems* (**H1.5D, H2.5D, H1.5*D, H2.5*D**)

The hydrogels with the most appropriate properties were used for the encapsulation of an anti-inflammatory drug – diclofenac sodium salt, forming four drug delivery systems (**H1.5D, H2.5D, H1.5*D, H2.5*D**), all having the same amount of the encapsulated drug, but differing between them through the crosslinking degree. In order to create the premises for a homogenous encapsulation of **DCF**, the drug delivery systems were obtained by an *in situ* hydrogelation procedure of the **S1** and **S2** derivatives in the presence of diclofenac, according to a procedure already used in our group [35,36].

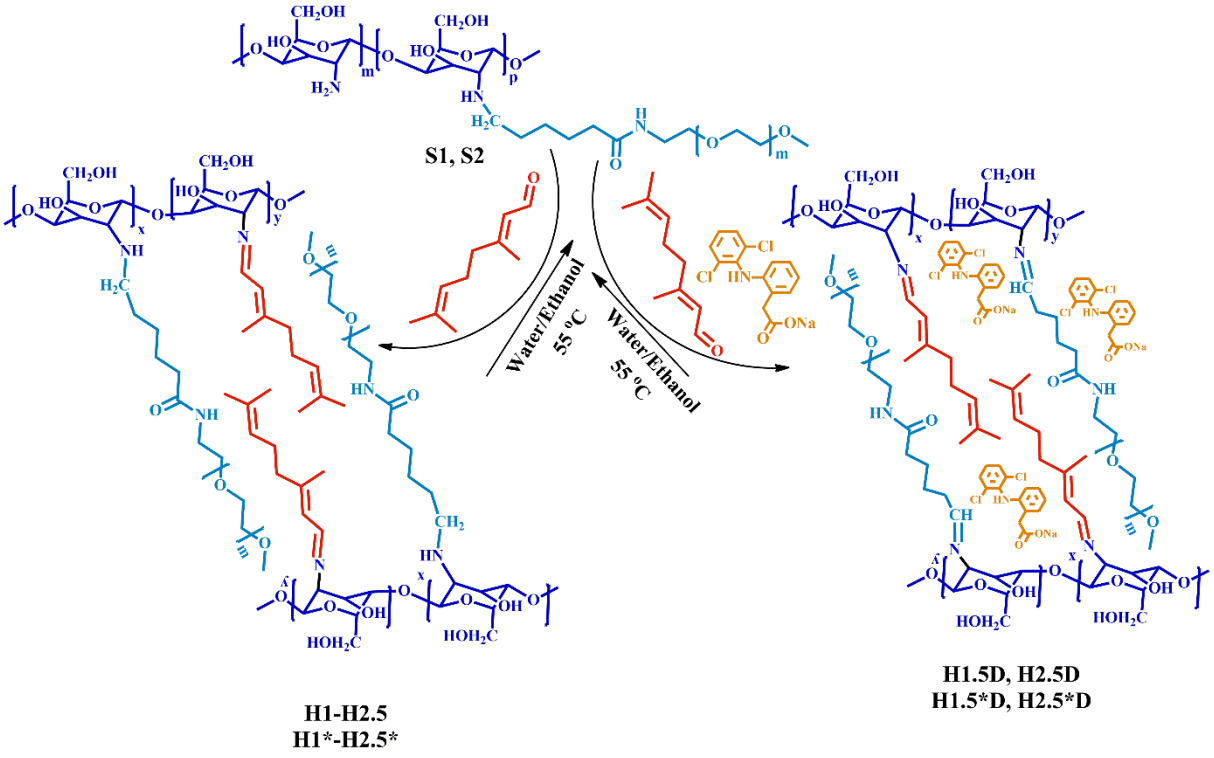

Scheme 1. Synthesis of the hydrogels

2.4 Methods

Freeze-drying. The xerogels and the drug delivery systems were obtained by their freezing in liquid nitrogen and further submission to freeze-drying of the corresponding hydrogels using a LABCONCO Free Zone Freeze Dry System equipment, in working conditions -54 °C and 1.510 mbar, for 24 hours.

ATR-FTIR spectra of the drug delivery systems (**H1.5D, H2.5D, H1.5*D, H2.5*D**), **DCF** drug and the hydrogels **H1-H2.5 and H1*-H2.5*** were recorded on the corresponding xerogels on a **FTIR** Bruker Vertex 70 Spectrophotometer equipped with a ZnSe single reflection ATR accessory. The measurements were performed between 4000–600 cm^{-1} range, with 32 scans and a resolution of 4 cm^{-1}. The overlapped bands from 1620-1480 cm^{-1} region in the FTIR spectrum of the drug delivery systems and of the blank xerogels were highlighted with the second derivative of the original spectra. The bands were deconvoluted using a curve-fitting assay, and the area of which peak was calculated with a 50% Lorentzian and 50 % Gaussian function. The curve-fittings were performed with the OPUS 6.5 and OriginPro 8 software. The obtained errors were lower than 0.003.

Wide angle X-ray diffraction (WAXD) of the samples was performed on a Bruker D8 Advance diffractometer at 36 kV and 30 mA, using Ni filtered Cu-Ka radiation (λ = 0.1541 nm). The diffractograms were recorded in the 2–40 degrees range, at room temperature, on pellets obtained by pressing a certain amount of sample using a hydraulic press (5 N/m^2).

The supramolecular characterization of the systems was realized by **polarized optical microscopy** (POM), using a Leica DM 2500 microscope.

The morphology of the samples was evaluated with a field emission **scanning electron microscope** (Scanning Electron Microscope SEM EDAX – Quanta 200) at accelerated electron energy of 10 eV. The morphological observations were carried out on xerogel samples, both for the hydrogels and formulations. The size of the pores and pore walls thickness was measured using the Image J Software.

The monitoring of the *in vitro* release kinetics was performed in phosphate buffer saline (PBS) (pH=7.4), at human body temperature, 37 ^{o}C. The obtained formulations (**H1.5D, H2.5D, H1.5*D, H2.5*D**) were used in the *in vitro* release experiments, following the further experimental procedure. Pieces of xerogels with a mass of 62 mg, containing 1.5 mg of **DCF** drug were immersed into 10 mL of PBS. At different time intervals, 2 mL of supernatant were withdrawn and replaced with new PBS, in order to keep the same volume and the same sink conditions. The concentration of the removed supernatant was determined by UV-vis spectroscopy, by measuring the absorbance of the characteristic absorption band of **DCF** at 275 nm and fitting on a calibration curve. The calibration curve was previously drawn by determining the absorbance for solutions of **DCF** with well-known concentrations and by the graphical representation of the absorbance as a function of concentration [37]. The cumulative drug release was calculated using the following mathematical equation:

$$\mathbf{\% \ DCF = [(10C_n + 2\Sigma C_{n-1})/m_o]x100} \qquad \text{Eq. 1}$$

where C_n and C_{n-1} represent the concentrations of the drug in the supernatant after n and

n-1 withdrawing steps, respectively, and m_0 = 1.5 mg, corresponding to the amount of **DCF** loaded in the samples. All the experiments were performed in triplicate and the values are given as the mean value for three independent measurements. The absorbance of the released **DCF** drug was measured using a Perkin Elmer Lambda 35 UV-Vis spectrophotometer.

The *in vitro release data* were analyzed by fitting the experimental data on the following well-known mathematical models:

***i) Zero order model*:** $Q_t = K_0 \cdot t$, where Q_t is the amount of drug dissolved in the time *t* and K_0 is the zero-order release constant.

***ii) Higuchi model*:** $Q_t = K_H \cdot t^{\frac{1}{2}}$, where Q_t is the amount of drug released in the time *t* and K_H is the Higuchi dissolution constant.

***iii) Hixson-Crowell model*:** $W_0^{1/3} - W_t^{1/3} = K \cdot t$, where W_0 is the initial amount of drug in the formulation, W_t is the remaining amount of drug in the formulation at time *t* and K is a constant.

iv) Korsmeyer-Peppas model: $\frac{M_t}{M_\infty} = K \cdot t^n$, where M_t/M_∞ is the fraction of drug released at the time *t,* K is the release rate constant and n is the release exponent.

***v) First order model*:** $logQ_t = log\ Q_0 + K \cdot t/2.303$, where Q_t is the amount of drug released in the time *t,* Q_0 is the initial amount of drug and K is the first order release constant.

The ***in vitro*** **enzymatic degradation** of the blank xerogels has been monitored by determining the mass loss of the xerogels in lysozyme buffer solution. With this aim, pieces of the xerogel **H2.5**, with a mass of 10 mg were added to 10 mL of lysozyme solution 10 mg/L and kept at 37°C [38]. The lysozyme solution was refreshed at every three days. At certain time intervals the pieces were took out, washed with double distilled water to remove the salts and submitted to analysis. A similar procedure was followed in order to evaluate the hydrolytic degradation of the samples, only in PBS solution. The mass loss determination was calculated using Equation 2 as follows:

$$\boldsymbol{W_{loss} = \frac{W_{0-} W_t}{W_0} \cdot 100} \qquad \text{Eq. 2}$$

where W_{loss}= the weight loss of the hydrogel

W_0= the initial weight of the xerogel

W_t= the weight of the xerogel at a predetermined moment

The investigations of the *in vivo* release kinetics were conducted on white Wistar rats (of 190-200g each) provided by the Grigore T. Popa University bio-base. The animals were kept in standard laboratory environmental conditions (with 12 hours/12 hours artificial periods

of light/darkness, a temperature of 22 ± 1°C and a relative humidity 55-65%). The rats were randomly assigned into 7 groups:

Group 1 (C): – control without pellets;

Group 2 (Cp): - implant with sterile cotton pellets – control with pellets;

Group 3 (DCF): implant with cotton pellets impregnated with DCF solution – positive control with diclofenac;

Group 4 (S1D): implant with pellets from **S1** grinded with DCF;

Group 5 (S2D): implant with pellets from **S2** grinded with DCF;

Group 6 (**H1.5D):** implant with **H1.5D** pellets;

Group 7 (H1.5*D): implant with **H1.5*D** pellets;

The rats received standard diet and water *ad libitum*, except during the time of the studies. Before the experiment, the rats were positioned on a raised wire mesh, under a transparent plastic cage and allowed, for two hours, to acclimate to the testing room. The sterile cotton pellets and the investigated sample pellets were administered by subcutaneous implantation. 12 hours before making the incision, the animals were food-deprived. The rats were generally anaesthetized, by intraperitoneal injection of ketamine (50 mg/kg body weight) and xylazine (10 mg/kg body weight), the dorsal region was shaved and antisepticised with 70% alcohol solution. A small incision was made in one dorsal area, the tested samples (weighting 62 mg) were inserted and the cut was sutured using a non-absorbable surgical thread. The pellets, similar as the foreign elements produced a local subacute inflammatory reaction.

The **somatic pain testing** was performed using tail flick assay (PanLAB Harvard apparatus) in order to evaluate the tail`s thermal nocifensive behavioral reaction, when the latency of nocifensive responses induced by thermal noxious tail stimulation was measured [J.S. Mogil, Animal models of pain: progress and challenges, Nat. Rev. Neurosci. 10 (2009) 283-294]. The measurements based on the fact that DCF has analgesic effect, and its release rate will induce a corresponding endurance effect to the pain. Using a standardized holder, the rats were gently held, being positioned with the tail above the heat source. Tail withdrawal latencies were recorded in response to thermal stimulus from a light beam concentrated on the dorsal surface of the tail (2 cm from the tip) [39]. When the rat moves its tail, the light beam initiates the photocell, disconnecting a switch, which turns off the radiant heat. The time taken for the animal to flick the tail away from the thermal stimulus, signifying the latency time of reactivity (seconds), was assessed [40,41].

The tail-withdrawal reactivity was measured before implantation (baseline) and 1 hour, 3 hours, 1 day, 3 days and 7 days after the pellets subcutaneous administration. The recorded

baseline latency was 4.3 ± 0.2 seconds (mean ± standard deviation – S.D. of mean). A cut-off time of 12 seconds, was used to avoid the tail damage.

The discrepancies between the measured and baseline latencies are appreciated as an index of antinociception. In this somatic pain model, the prolongation in the time for the rat to move its tail is indicative of analgesia, while, the reduction in the tail-flick latency are suggestive for hyperalgesia [40,42].

The latency data from tail withdrawal measurements were converted to per cent of maximum possible effect (%MPE) using the equation [43].

%MPE = [(measured latency-baseline latency)/(cut off time-baseline latency)] × 100 Eq.3

The ***in vivo*** **biocompatibility** of the implanted pellets was evaluated by assessing their influence on some hematological, biochemical and immune parameters. 24 hours and 7 days after the pellets administration, under general anesthesia, the blood was collected from the retro orbital plexus and the following parameters were investigated: leukocyte formula (polymorphonuclear neutrophils - PMN, lymphocytes - Ly, eosinophiles - E, monocytes - M, basophils - B), the activity of liver enzymes (aspartate aminotransferase (AST), alanine aminotransferase (ALT), lactate dehydrogenase (LDH)) and, phagocytic capacity of peripheral neutrophils (NBT test) and serum complement activity [45]. The NBT test and the serum complement activity are specific parameters of a battery test used to investigate the immunologic effects of pharmacological active substances in laboratory animals [46,47].

The data were expressed as mean +/- standard deviation (S.D.) and processed using SPSS version 17.0 for Windows 10, to estimate the differences between control groups and the groups receiving the subcutaneous pellets, with or without diclofenac. The values of *p* (probability) coefficient below 0.05 were considered to be statistically significant comparing with those of the control group.

The protocol of the experiments and the surgical procedures were approved by the University Committee for Research and Ethical Issues, according to the regulations of the IASP Committee for Research and Ethical Issues, in compliance with the international guidelines, regarding the handling of laboratory animals [48-50].

Results and discussions

New hydrogels with improved hydrophilicity were obtained by the acid condensation of two amino-PEG-ylated chitosan derivatives with citral monoaldehyde, and were further used as matrix for the encapsulation of an anti-inflammatory drug – diclofenac sodium salt (Scheme

2). The amino-PEG-ylated chitosan derivatives were obtained by reductive amination of the imino-PEG-ylated chitosan ones. Hydrogels based on chitosan and citral have already proved *in vivo* biocompatibility on rats and were also successfully used as matrix for anticancer drug delivery [26,35]. These systems presented important characteristics which made them suitable for bioapplications, but their high hydrophobicity led to low performances when used in drug delivery [36]. Therefore, we proposed the use of PEG-ylated chitosan as starting polymers for the obtaining of citryl-imino-chitosan hydrogels with improved properties, closer to the standards imposed for bioapplications.

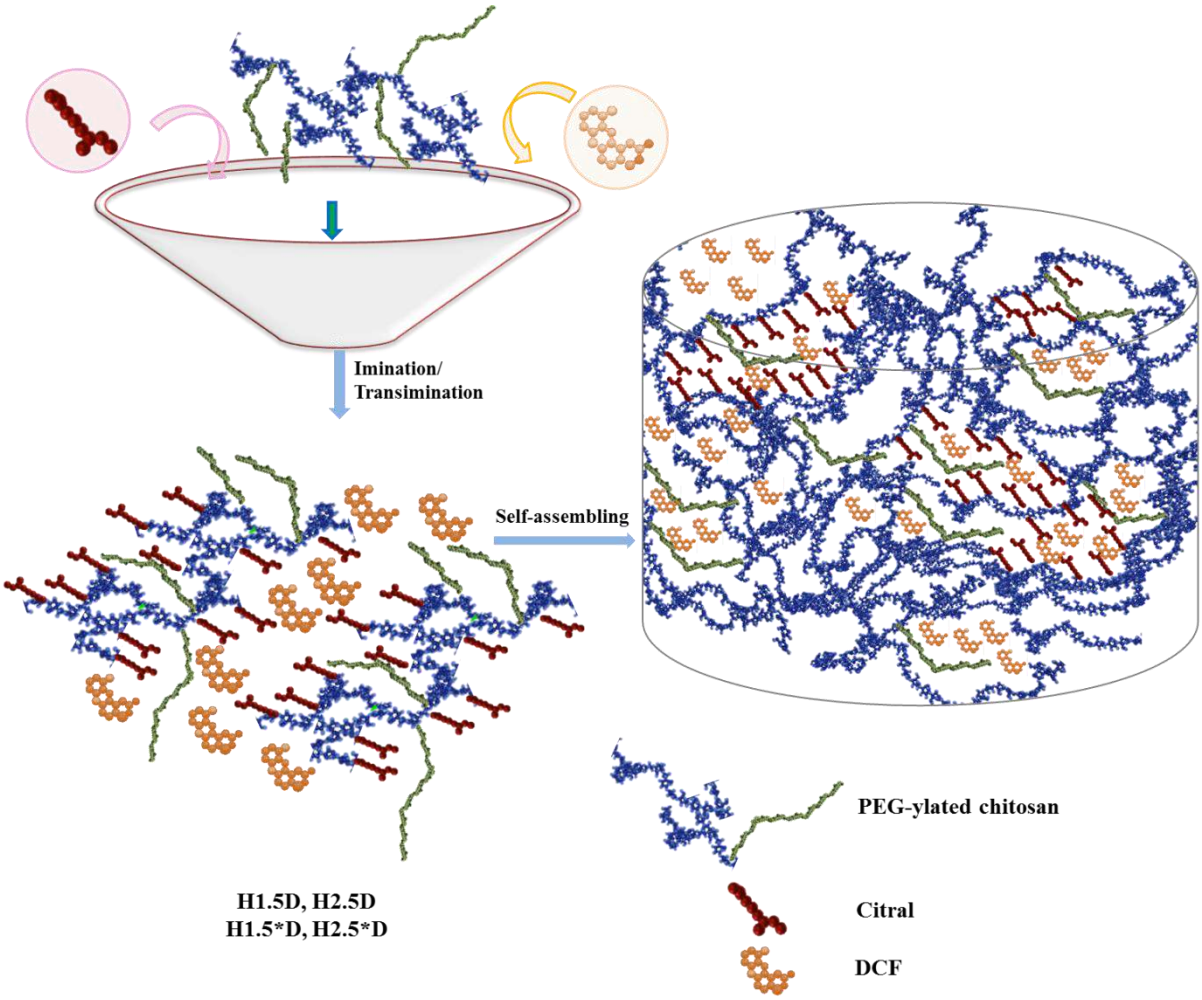

Scheme 2. The obtaining of the drug delivery systems

3.1 Structural characterization by FTIR

FTIR spectroscopy was used in order to characterize the PEG-ylated chitosan derivatives used as precursors and the hydrogels and drug delivery systems. For comparison, the FTIR spectra of the pristine chitosan and of PEG-aldehyde were also recorded.

The successful obtaining of the PEG-ylated chitosan derivatives was confirmed by some changes which occurred in the fingerprint region of the FTIR spectra. Therefore, the maximum of the broad peak from 1635 cm^{-1} in chitosan's spectrum shifted at first to 1642 cm^{-1} in the **D1,**

D2 imino-chitosan derivatives (See Figure S1). Next, due to the imine reduction (**S1**, **S2**), the maximum of this peak shifted to higher wavenumbers, at 1658 cm^{-1}, indicating the dominance of the amide groups from PEG-aldehyde structure in the detriment of the imine ones, consumed by reductive imination (See Figure S1). These data were observed even better by the deconvolution of the peaks in discussion (See Figure S2). Further, the success of citral grafting on PEG-ylated chitosan derivatives was demonstrated by the shifting of the maximum from 1658 cm^{-1} to 1645 cm^{-1} confirming the formation of new imine linkages between the amino groups of **S1** and **S2** derivatives and citral [26, 35]. This new peak is quite broad and by its deconvolution was observed that it is actually formed by the superposing of three individual peaks as follows: at 1638 cm^{-1} the stretching vibration of the amine group from chitosan, at 1645 cm^{-1} the one corresponding to the newly formed imine and at 1661 cm^{-1}, which is actually the amide group from PEG-aldehyde, which slightly shifted due to hydrogen bond formation. (See Figure S3). As expected, the CH=N band appeared at quite high wavenumbers, in agreement with the lower degree of conjugation of the imine linkage between two aliphatic units, as previously reported [26, 50]. Moreover, simultaneously with this change which indicated the formation of imine band, the stretching vibration of the CH=O group from the citral spectrum (1675 cm^{-1}) significantly diminished in intensity indicating its consumption (Figure 1).

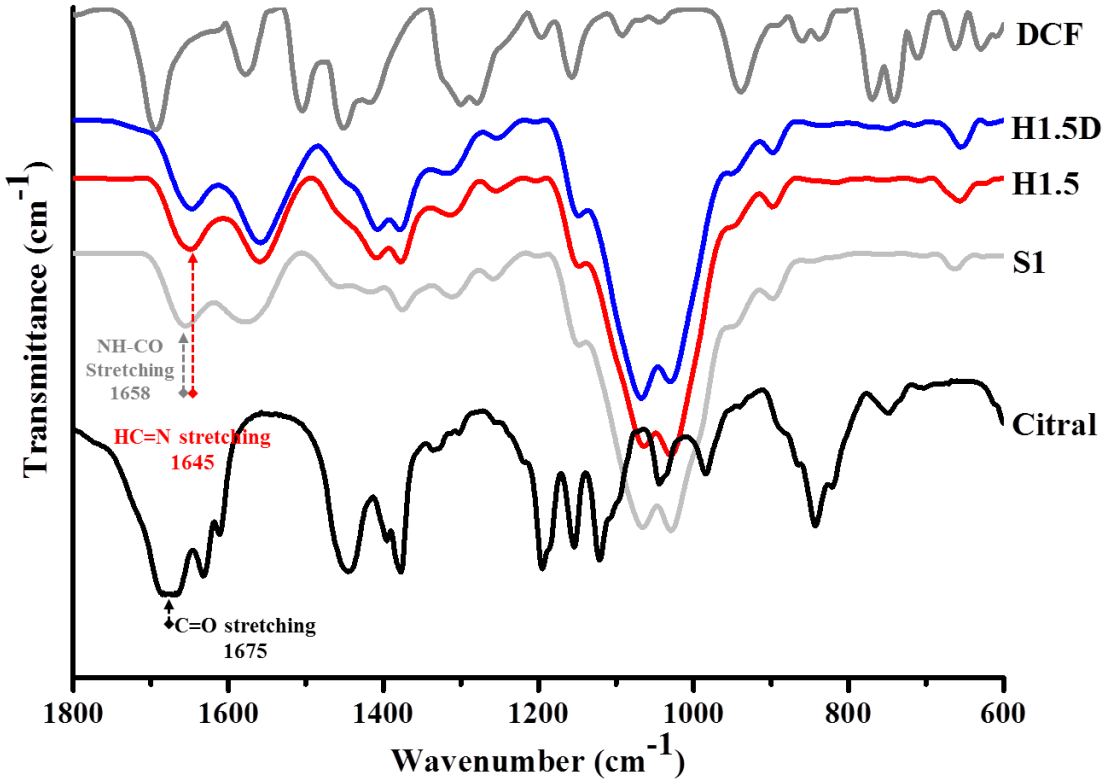

Figure 1. FTIR spectra of some representative drug delivery systems and the blank hydrogels

By comparing the FTIR data of the drug delivery systems with the ones of the blank hydrogels, no band from the drug could be clearly observed. However, by the deconvolution of the spectral region between 1620-1480 cm^{-1}, a band which corresponds to the groups stretching vibrations of the C=O from DCF drug appeared, indicating its successful encapsulation (See Figure S3).

3.2 Supramolecular characterization by WXRD

Wide angle X-ray diffraction was used in order to (i) determine the supramolecular architecture of the PEG-ylated chitosan-based hydrogels and to (ii) evaluate the state of the encapsulated drug into the formulations.

The PEG-ylated chitosan derivatives based either on imine or amine linkages maintain in their supramolecular arrangement, the morphological peculiarities of both components: chitosan and PEG presenting a broad band with two maxima from chitosan, at 12 and 21 dgr and two maxima from PEG-aldehyde at 19.7 and 23.3 dgr (See Figure 4S) [51, 52].

The diffraction pattern of the hydrogels on the other side, changed in terms of peaks shape and position, but remains similar to the previously reported ones for hydrogels based on chitosan and monoaldehydes [21-26]. Therefore, the diffractograms indicated a layered supramolecular architecture, due to the same hydrogelation mechanism, consisting in hydrophilic-hydrophobic segregation, along with the formation of highly ordered hydrophobic clusters between the imino-citryl moieties. This was evidenced by the new peak from 4.2 dgr, which corresponds to a distance of 21 Å (Figure 2) between the hydrophobic and hydrophilic layers, similar to other cases previously reported by our group [15-20]. Concerning the other reflections in the xerogels diffractograms, some changes could be also observed due to the hydrogelation process, and also due to the PEG presence: (i) the peak from chitosan which appeared at 20.1 dgr, became sharper, sign of the increased degree of ordering in the xerogels (ii) the peak from 13.5 dgr moved to smaller angles in the diffractograms of the xerogels (at 12.28 dgr), therefore to higher distances very probably because of the PEG side chains which keep apart the chitosan chains within the same layer (iii) a new peak appeared at 8.5, 2 theta dgr, possible attributable to PEG ordering among imino-chitosan chains.

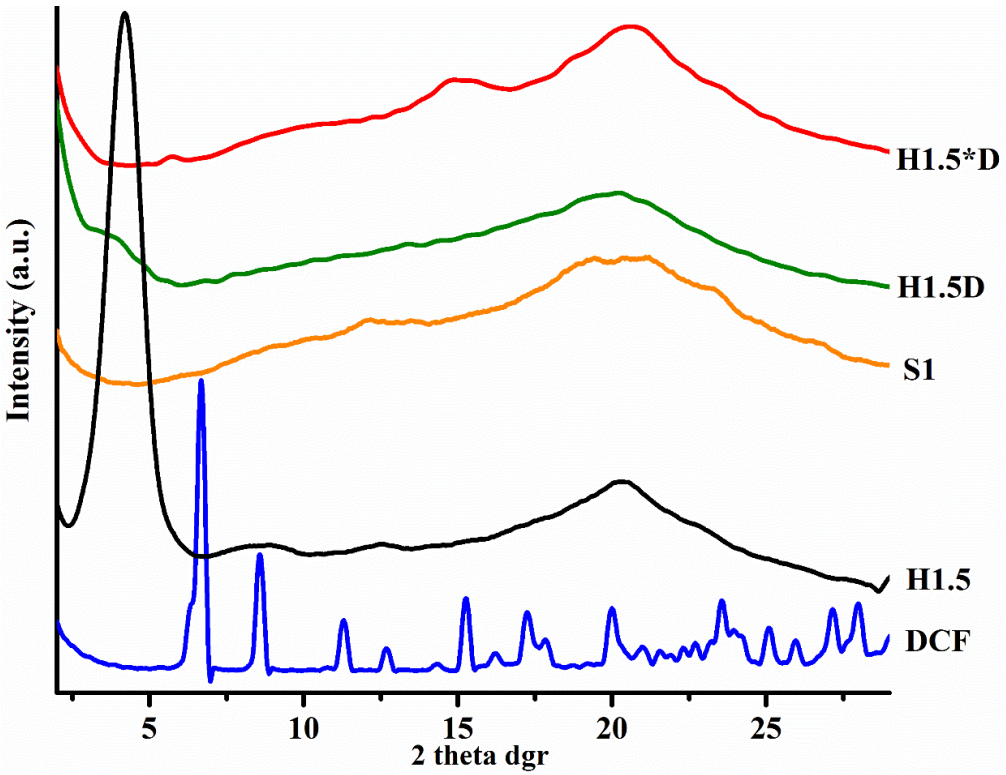

Figure 2. X-ray diffractograms of some representative drug delivery systems, blank hydrogels and their components

Regarding the supramolecular arrangement of the drug delivery systems some notable differences could be observed in comparison to the blank hydrogels. At first, it seems that the drugs presence hindered somehow the hydrophobic hydrophilic segregation of the citryl-imino-chitosan derivatives, fact evidenced by the almost disappearance of the reflection from the small angles domain. Secondly but equally important, the matrix seams to prevent the crystallization of the DCF drug, very probably due to the high viscosity of the system. As it could be observed, no evident reflections characteristic to DCF could be observed in the diffractograms of the drug delivery systems. This means that the drug is dispersed at sub-micrometric level in the hydrogel matrix, due to the strong interactions established between them.

The high degree of ordering of the xerogels was confirmed by polarized optical microscopy (POM). Therefore, in polarized light, all the samples presented birefringence (Figure 3 and Figure 5S), which is similar to the one characteristic to the layered mesophase of smectic liquid crystals [53,54]. Moreover, a slightly difference in terms of birefringence intensity could be observed for the systems containing the drug and the ones without the drug. Therefore, the drug delivery systems are less intensely colored than the blank hydrogels, sign of their lower degree of ordering, finding which is in agreement with the X- ray data.

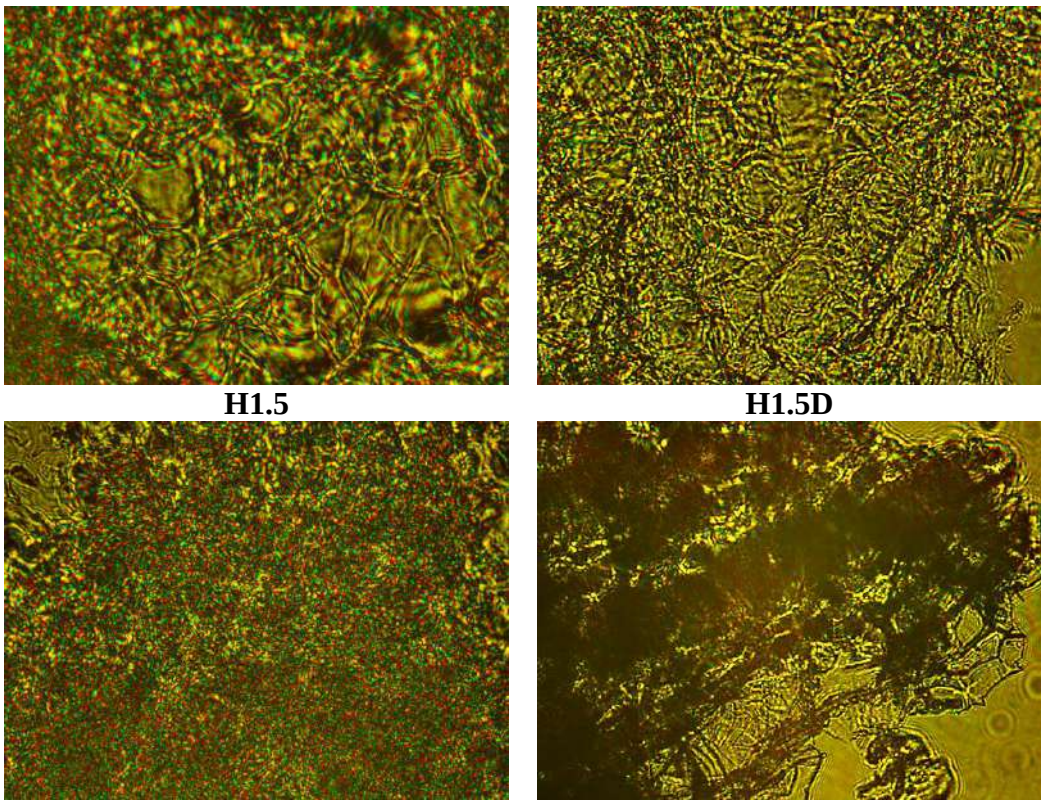

Figure 3. Polarized optical microscopy images of some representative xerogels

3.3 Morphological characterization by SEM

The morphological investigations by SEM revealed quite important differences in the microstructure of the xerogels, clearly because of the different PEG content. Therefore, the xerogels based on the chitosan derivative which contains more PEG (**H** series), presented a porous microstructure with fibrous aspect (Figure 4 and Figure 6S). On the other side, the xerogels obtained using the chitosan derivative with less PEG, presented a clearer porous morphology, but with smaller pores in comparison with chitosan based xerogels without PEG [26,35]. The drug delivery systems on the other side, regardless the PEG content, exhibited a porous morphology, with micrometric pores with thicker walls (walls thickness ~9-13 μm). More than this, the aspect of the xerogels is more robust, indicating that the encapsulation of the drug occurred mainly inside the pores walls. No micrometric drug crystals were observed into the xerogel mass, confirming once more that the drug was encapsulated at sub-micrometric level into the xerogels pores walls, as was demonstrated by POM and X-ray diffraction data.

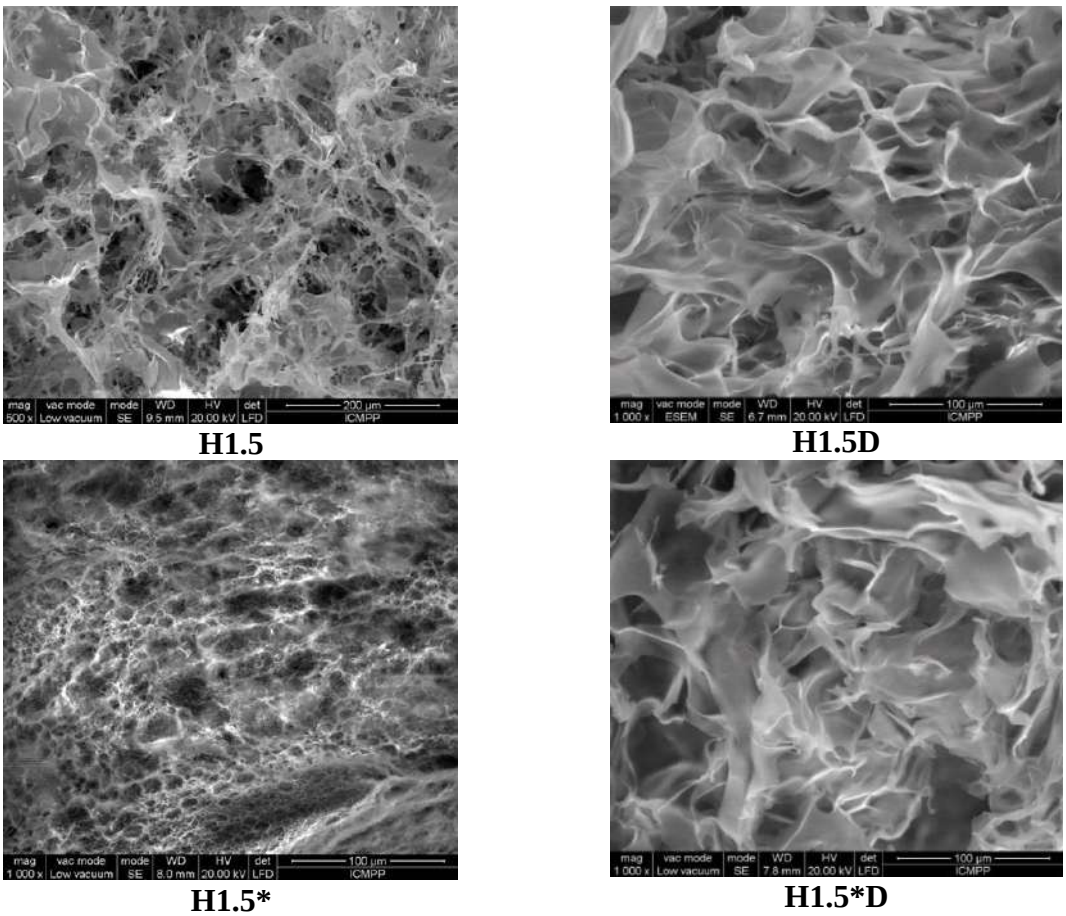

Figure 4. SEM microphotographs of some representative xerogels and drug delivery systems

3.4 Swelling behavior

The swelling ability of the xerogels was investigated by determining the mass equilibrium swelling (MES) in two media with different pH: (i) phosphate buffer saline (PBS) with a pH of 7.4, similar to the one of biological tissues; (ii) water with neutral pH (Figure 5).

In both media, the xerogels were able to rehydrate fast, forming hydrogels with high water content in less than one minute. Moreover, the obtained values of the MES depended mainly on the content of hydrophilic PEG from the chitosan-*g*-PEG derivatives. As expected, the xerogels obtained using the **S1** (the one which contains the higher amount of PEG) derivative presented a higher ability of swelling and led to higher values for the MES parameter, reaching a maximum of 120% in water and 54% in PBS in only 4 hours for **H** series and 6 hours for the **H*** series. On the other side, the xerogels obtained using the **S2** derivative presented lower values of the MES in both water and PBS (100 and 46%, respectively) but still higher in comparison with the ones obtained for hydrogels based on citryl-imino-chitosan (28 % and 7.5 %, respectively) [26]. This behavior can be explained if we take into consideration the influence of PEG, a highly hydrophilic polymer known for its ability to swell and retain large amount of water [55].

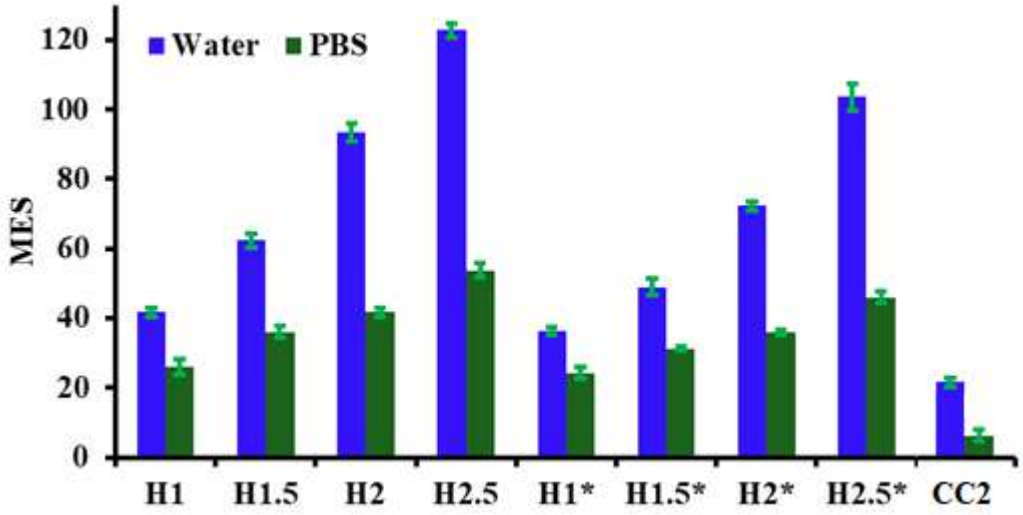

Figure 5. Mass equilibrium swelling for the blank xerogels and a reference sample based on citryl-imine chitosan xerogel (Apare CC2?, poate e bine sa il explicit (CC2 is the reference hydrogel based on citryl-imino-chitosan)

3.5 *In vitro* drug release

The release kinetics profile was monitored *in vitro* in phosphate buffer saline with a pH close to the physiological one (pH=7.4), at human body temperature (37 ^{o}C) for all samples. The understudy drug delivery systems were able to release the encapsulated DCF drug with different rates depending mainly on their ability to absorb water. Still, by analyzing the release profiles of the samples, two release stages could be observed, well correlated with the swelling behavior of the matrix. The hydrophilicity of the systems generates complex macromolecular and supramolecular changes in the polymeric network under the influence of water molecules. Therefore, the samples with higher PEG content (**H1.5D** and **H2.5D**), characterized by higher mass equilibrium ratios and further higher hydrophilicity, due to their fast swelling (reaching the MES in 4 hours), higher volume expansion and further elasticity of the network released the encapsulated drug faster. On contrary, the samples with lower PEG content released the **DCF** with a slower rate. Differences in terms of percentage cumulative drug release were also noticed. After 7 days, the most hydrophilic sample, **H2.5D**, released almost the entire amount of the encapsulated drug (~99.5%), while the less hydrophilic one, **H1.5*D** released only 91%. These differences can be explained if we take into consideration the hydrophilicity, but also the elasticity of the networks, under the influence of water, due to the different crosslinking degree. Thus, the **H1.5*D** sample contains a lower amount of PEG and a higher amount of citral, which led to a more compact and rigid network, with stronger and denser crosslinking nodes, which will hinder the drugs diffusion. By comparing the **DCF** release data obtained in this cases with

previously reported work, it could be observed a more obvious sustained release in our case, the systems being able to release the encapsulated drug up to 168 hours [56-59].

Table 1. *Cumulative % DCF release from chitosan based materials*

System	Cumulative DCF release at 4 hours	Cumulative DCF release at 8 hours	Cumulative DCF release at 24 hours	Reference
Citryl-imine-PEG-ylated chitosan hydrogels	23.3 %	30.59 %	39.59 %	This study
Xylan/chitosan complexes based hydrogels	>95 %	> 95 %	> 95 %	56
Nitrosalicyl-imine-chitosan hydrogels	~ 20 %	~ 25 %	~ 40%	36
Alginate Microspheres encapsulated in chitosan hydrogels	~ 38 %	~ 55 %	~ 80 %	57
Chitosan-N-isopropylacrylamide hydrogels	>40 %	>50 %	>50%	58
Chitosan-g-poly (acrylic acid)/attapulgite/sodium alginate composite hydrogel	>90 %	>90 %	> 95%	59

Moreover, even if a burst effect was observed, the cumulative % drug release at 4 hours being ~ 23%, in other systems the burst effect is significantly higher, the cumulative % drug release reaching even values of 95% [55]. However, the drug release profiles, regardless the samples content, are characteristic to the systems with sustained release, with a burst effect in the first 4 hours, when a shock dose is necessary, followed by a quite large interval in which the therapeutic dose is kept constant (up to 7 days) [57]. Therefore, it can be concluded that the citryl-imine-PEG-ylated chitosan hydrogels are adequate for both acute pain treatment (due to the burst release effect) but also to the rheumatic chronic pain, due to their ability to release the encapsulated **DCF** up to 168 hours. This is definitely attributed to the strong physical interactions (especially hydrogen bonds) which can be established between the **DCF** drug and the imino-PEG-ylated chitosan hydrogels.

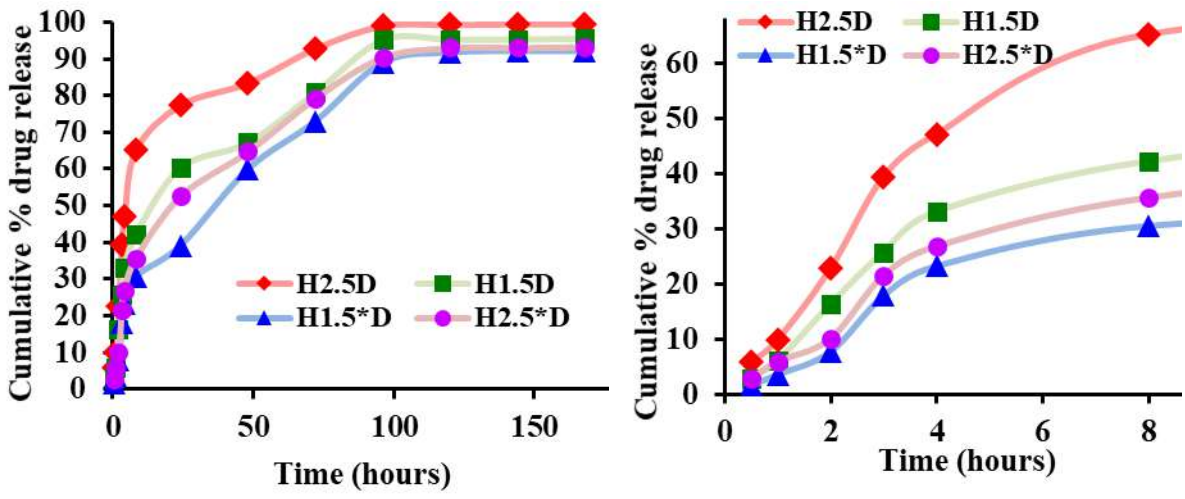

Figure 6. Drug release kinetics for the drug delivery systems (a) for 7 days and (b) for 8 hours

3.6 The analysis of drug release kinetics

Diclofenac sodium salt is a hydrophilic drug, whose release from any formulation may be governed by multiple factors, such as diffusion, solubility, matrix swelling or even erosion [48]. Moreover, due to the intrinsic chemical structure of the DCF, containing two chlorine atoms, one esteric group and one nitrogen atom is possible to create the ground for the development of physical interactions with the PEG-ylated chitosan matrix, which will also influence the release mechanism [60].

Therefore, aiming to elucidate and to draw a scenario regarding the mechanism of DCF release from the imino-PEG-ylated chitosan matrix, the *in vitro* release data were fitted to different mathematical models: Zero Order, First order, Korsmeyer-Peppas, Higuchi and Hixson-Crowell. The mathematical models were applied on the both stages (i) from 30 min to 4 hours and (ii) from 8 hours to 96 hours (Table 2,3).

In the first release stage, the straight line obtained in the case of the zero order model, with high values of the correlation coefficient (0.98-0.99) proves that the release of the DCF from the xerogels occurs with constant rate, fact which may increase the bioavailability of the drug and also may prolong its pharmaceutical action [50]. The differences in terms of k_0 constant values show the slight influence of the hydrophilicity of the matrix on the drug release rate. Moreover, the good fitting of the zero order model on the kinetic data revealed the importance of DCF dissolution on the release process from the citryl-imino-PEG-ylated chitosan xerogels [61].

The good fitting of the first order model, (correlation coefficient: 0.97-0.99), showed the significant influence of the amount of DCF encapsulated on the amount of DCF released [62,63].

The Higuchi model, on the other side, fitted quite well (R^2=0.98 for the xerogels based on **S1** derivative and R^2=0.94 for the xerogels based on **S2** derivative), showing that the DCF release from the matrix is also controlled by the diffusion through the xerogel matrix. Beside this, the fitting of the Hixson Crowell model with high values of the correlation coefficient (0.99-0.97) indicated the prevalence of the DCF dissolution on its diffusion. In order to have information regarding the type of diffusion, the Korsmeyer-Peppas model was used. The n_r values which are higher than 1, for all samples indicated a nonFickian supercase of transport 2, characteristic to the systems in which the erosion of the matrix plays an important role [61].

Table 2. *The data obtained by fitting the kinetic data on different mathematic models for the first stage (1-4 h)*

Code	Zero order		First Order		Higuchi model		Hixson-Crowell		Korsmeyer-Peppas		
	R^2	K_0	R^2	K_t	R^2	K_H	R^2	κ	R^2	k	n_r
H2.5D	0.99	12.5	0.99	0.172	0.97	33.77	0.99	-0.24	0.99	1.049	1.055
H1.5D	0.99	8.91	0.99	0.108	0.98	24.1	0.99	-0.15	0.99	0.817	1.26
H2.5*D	0.98	7.11	0.97	0.082	0.94	19.03	0.97	-0.12	0.98	0.76	1.09
H1.5*D	0.98	6.45	0.97	0.073	0.93	17.17	0.97	-0.1	0.99	0.58	1.28

R^2: correlation coefficient; K: proportionality constant; n: release exponent

In the second stage of the process, the fitting of the *in vitro* kinetic data on the same mathematic models show high correlation coefficient values for Zero Order, Higuchi, Hixson Crowell and Korsmeyer Peppas models. This revealed that the mechanism of release is not significantly affected in time. Though, a big difference in the values of the n_r parameter from the Korsmeyer Peppas model was observed indicating changes in the drug diffusion mechanism, from nonFickian supercase 2 in the first stage (n_r>1) to quasi Fickian in the second one (n_r<0.45) [63,64]. Differences in the values of the proportionality constants in the two different stages were also observed, in all cases the k values being much higher in the first stage, in comparison to the stage 2.

This being said, it can be concluded that the release of the DCF drug from the citryl-imino-PEG-ylated chitosan xerogels is a complex process, governed by both drug and matrix peculiarities through different but equally important factors: i) drugs dissolution, ii) drug diffusion, iii) matrix swelling, iv) matrix erosion.

Table 3. *The data obtained by fitting the kinetic data on different mathematic models for the second stage (8-72 h)*

Code	Zero order		First Order		Higuchi model		Hixson-Crowell		Korsmeyer-Peppas		
	R^2	K_0	R^2	K_t	R^2	K_H	R^2	κ	R^2	k	n_r
H2.5D	0.97	0.36	0.89	0.037	0.99	4.72	0.96	-0.02	0.98	1.66	0.162
H1.5D	0.97	0.55	0.89	0.025	0.98	7.13	0.94	-0.02	0.97	1.345	0.307
H2.5*D	0.98	0.6	0.97	0.02	0.99	7.73	0.98	-0.02	0.99	1.21	0.36
H1.5*D	0.99	0.67	0.95	0.018	0.98	8.48	0.99	-0.02	0.96	1.05	0.43

R^2: correlation coefficient; K: proportionality constant; n: release exponent

3.7 *In vitro* enzymatic degradation

Enzymatic biodegradability is an important requirement for a material used for *in vivo* bioapplications, especially in drug delivery. That is why, the enzymatic degradation of some representative citryl-imino-chitosan xerogels has been investigated in the presence of lysozyme. The experiments were carried out at physiological pH, at human body temperature, 37 ^oC in order to mimic the biological environment [64]. The enzymatic degradation was monitored quantitatively and qualitatively by determining the mass loss and also the morphological changes by SEM. By comparing the mass loss of the **H2.5D** drug delivery system with the one of the blank xerogel **H2.5**, no significant changes could be observed, indicating that DCF encapsulation doesn't influence in a significant manner the matrix erosion [36]. Very interesting, despite the fact that the mechanism of lysozyme action involves the presence of two N-acetyl sites [36, 65], very high values of the mass loss were obtained (a maximum of 46% after 21 days was achieved), much higher than the one expected for a chitosan with such a low N-acetylation degree as the one used in this study. Therefore, it could be concluded that the matrix suffers also hydrolytic erosion, not only the cleavage of the C-O-C linkages between two N-acetylated glucosamine units caused by lysozyme presence. In order to evaluate the extent of the hydrolytic erosion of the xerogel, the degradation was also monitored in the absence of lysozyme, only in PBS solution [35,36]. Much lower values for the mass loss were obtained in this case, reaching a maximum of 24.7% after 5 days (in comparison with 32.6% in the presence of lysosyme), after which no further mass loss occurred. Though, even if the hydrolytic degradation didn't reach the extent of the enzymatic one, it reached high values in comparison to other systems previously studied in our group [35,36]. This can be easily explained if we take into consideration the increased hydrophilicity of these systems, due to the PEG's presence.

The SEM microphotographs of the samples which suffered enzymatic degradation showed ruptures in the xerogels pores walls even after 24 hours (Figure 7 b). Later, after 3 or

more days, the morphology was affected even more, the pore walls becoming tattered, leading to the complete loss of the pristine morphology (Figure 7 c, d).

Therefore, the understudy systems are easily bio-erodible, a major requirement for *in vivo* bio-applications in drug delivery and not only. Moreover, the systems are versatile from this point of view, the rate of erosion being quite controllable and influenced in a major manner by the hydrophilicity and therefore, crosslinking degree.

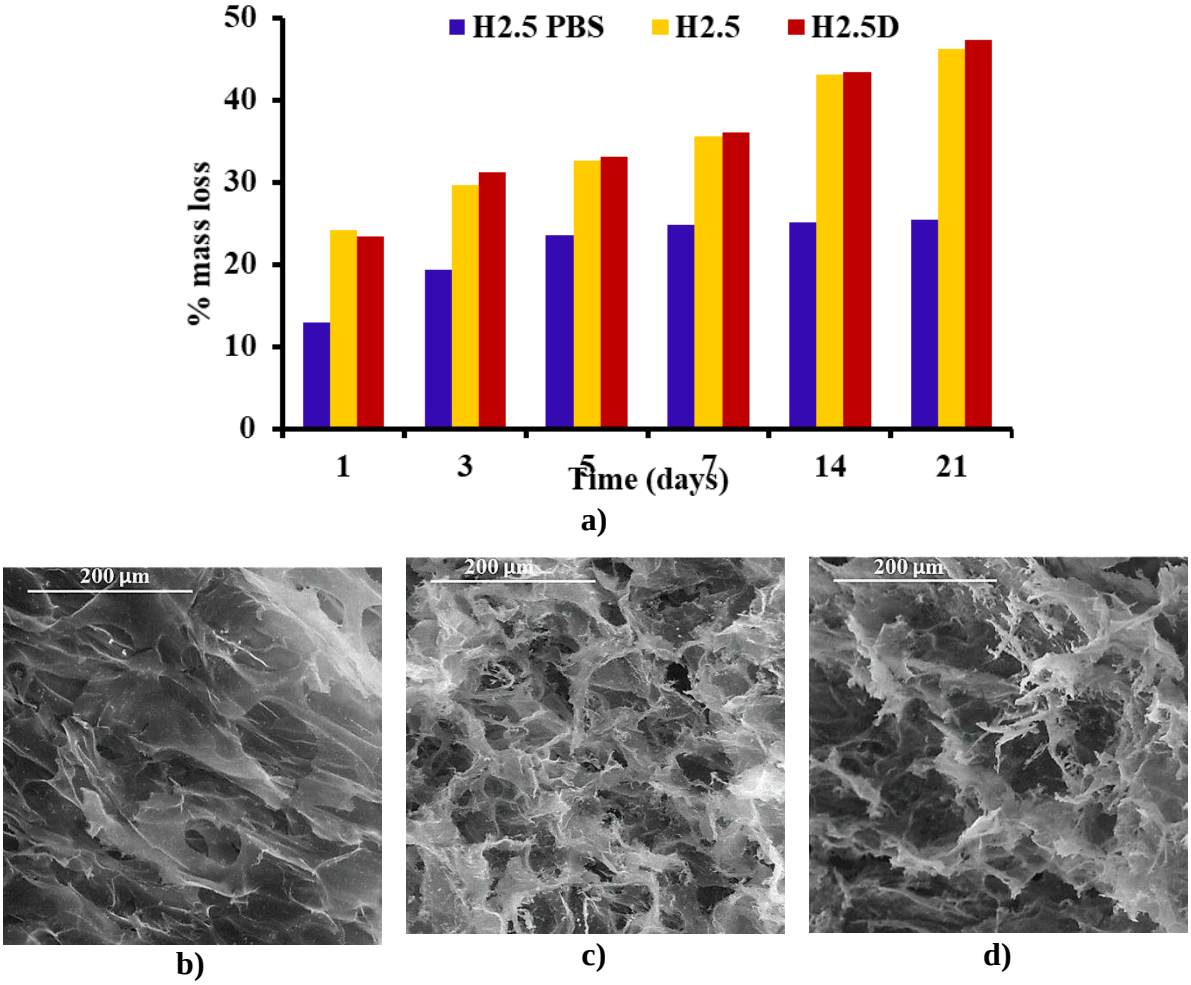

Figure 7. Graphical representation of the mass loss *versus* time (a) and some representative SEM images at different time intervals 1 day (b), 3 days (c), 21 days (d)

3.8 *In vivo* biocompatibility evaluation

The *in vivo* biocompatibility of the drug delivery systems (**H1.5D**; **H1.5*D**) and of the blank samples (**S1D** and **S2D** which represent physical mixtures of the two PEG-ylated chitosan derivatives S1 and S2 with DCF drug) was monitored by evaluating their influence on some hematological, biochemical and immune systems parameters. At 24 hours and 7 days after administration, were investigated: leukocyte formula (polymorphonuclear neutrophils - PMN, lymphocytes - Ly, eosinophils - E, monocytes - M, basophils - B), aspartate aminotransferase

(AST), alanine aminotransferase (ALT), lactate dehydrogenase (LDH), phagocytic capacity of peripheral neutrophils (NBT test) and serum complement activity [44]. Control samples were used as follows: positive control samples which were cotton pellets impregnated with saline solution (**Cp**) or diclofenac (**DCF**) and negative control samples which were treated only with saline solution (**C**).

By comparing the leukocyte formula of the rats which were treated with sterile cotton pellets (**Cp**) to the one of the control group without implant (**C**), it could be observed that the white blood cell differential counts exhibited an important percentage increase of the PMN (**p<0.01), M (**p<0.01) and B (**p<0.01) parameters, while the lymphocyte (**p<0.01) percentage decreased, indicating an inflammatory process.

The subcutaneous administration of pellets impregnated with DCF (**DCF**), on the other side, was associated with the substantial decrease of the peripheral PMN (♦p<0.05), M (♦♦p<0.01), B (♦♦p<0.01) percentages and an increase of the Ly (♦p<0.05) percent, statistically significant compared to the control group with implant, after 24 hours during the experiment.

In animals from the groups 4 and 5 (**S1D**; **S2D**), which received pellets obtained by simply mixing the PEG-ylated chitosan derivatives with DCF, the blood tests showed a diminution in the percentage of PMN (♦p<0.05), M (♦♦p<0.01) and a rise in the percentage of Ly (♦p<0.05), statistically significant 7 days after the subcutaneous implantation of the understudy compounds. These effects on the white blood cells were less accentuated than the one of the **DCF** group. The use of the pellets in groups 6 and 7 (**H1.5D**; **H1.5*D**) resulted in a decrease of the PMN (♦p<0.05) and of the M (♦p<0.05) percent and an increase of the Ly (♦p<0.05) percent, statistically significant compared to the control group with implant (**Cp**), only at 7 days after the substances administration. Their influence on the serum percentage of these blood cells was less intense than of the group with pellets impregnated with DCF in the experiment. The effects of the tested substances on the elements of the leukocyte formula were in a descending order as follows: **DCF > H1.5D > H1.5*D > S1D > S2D**.

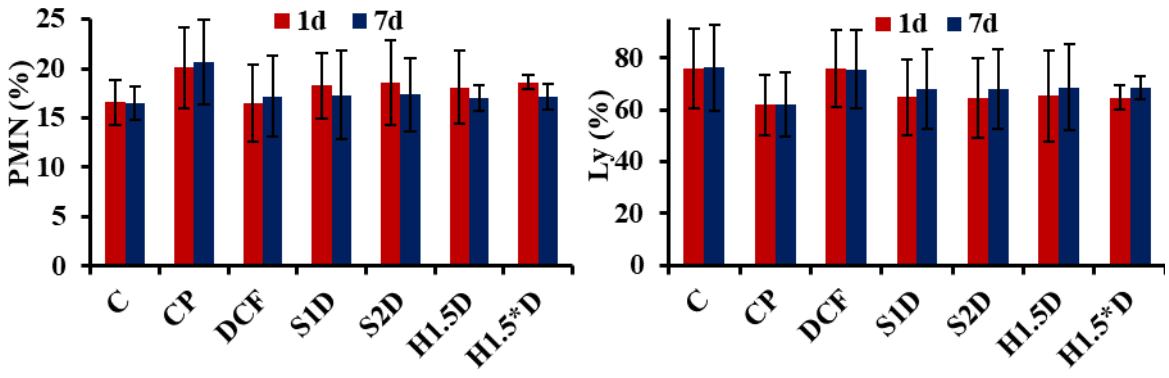

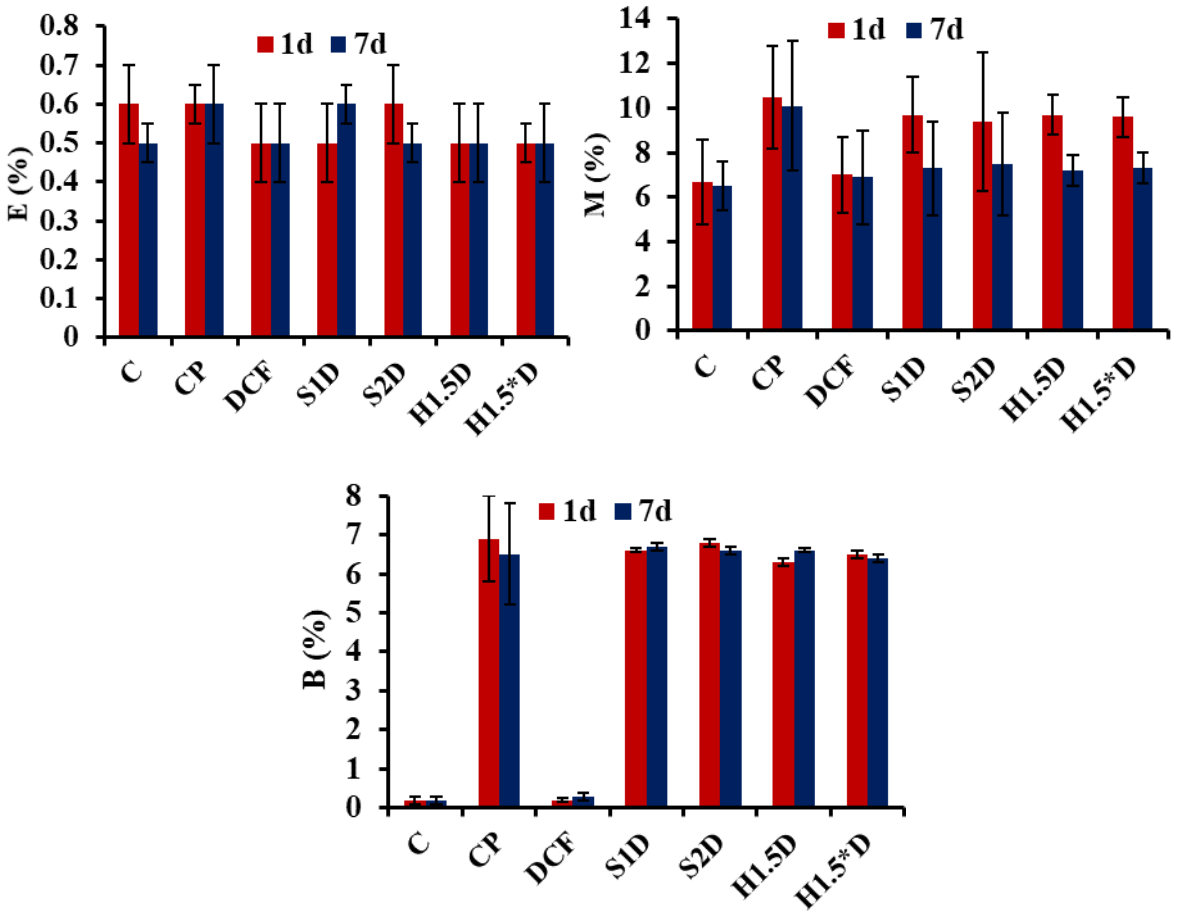

Figure 8. The modifications of the differential white cell count after subcutaneous implantation of the pellets. Values were presented as mean +/- S.D. for 6 animals in a group. *p<0.05, **p<0.01 (*vs* control), ♦p<0.05, ♦♦p<0.01 (*vs* control pellets)

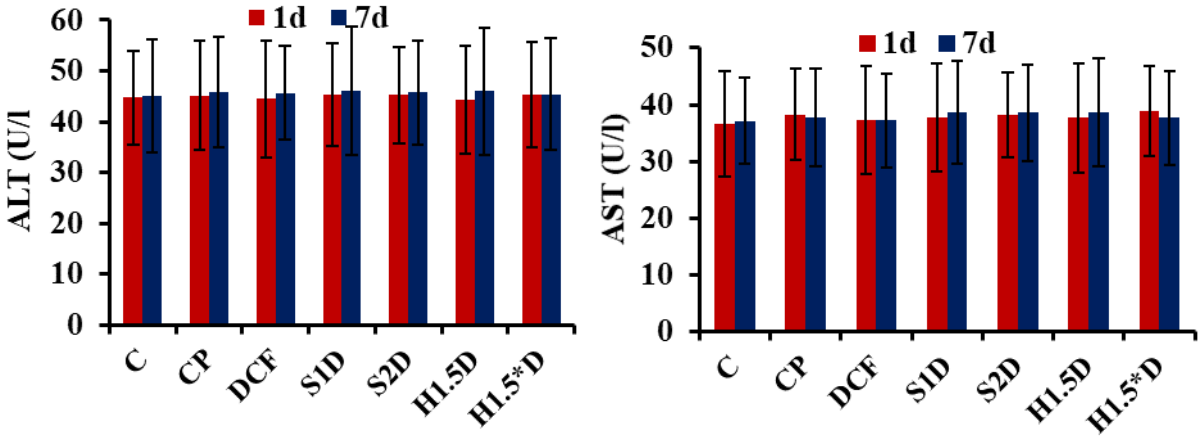

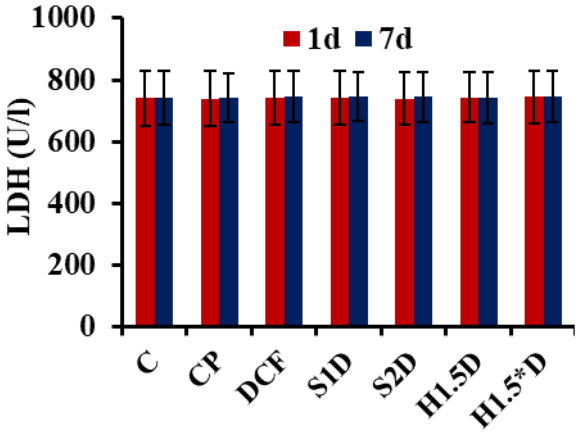

Figure 9. The modifications of the liver enzymes activity after subcutaneous implantation of the pellets. Values were presented as mean +/- S.D. for 6 animals in a group.

No considerable differences in the ALT and AST activity between the groups 3, 4, 5, 6, 7 and the control groups with or without pellets have been revealed, after 24 hours, nor after 7 days in the experiment.

Biochemical analysis hadn't shown any substantial variations in the plasmatic level of LDH, in rats from the groups 3, 4, 5, 6, 7 and the control group without implant, as well as the control group with cotton pellets, at both moments of the determinations.

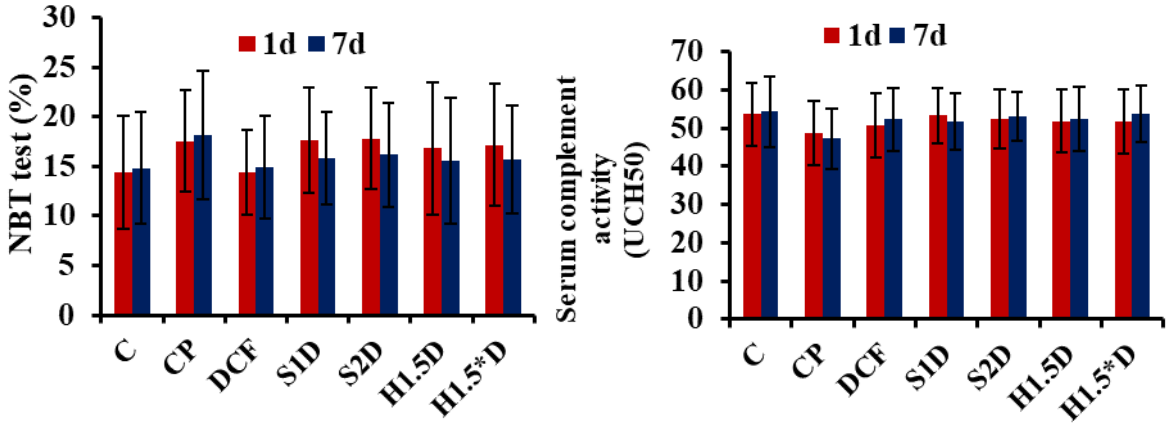

Figure 10. The modifications of some immune parameters after subcutaneous implantation of the pellets in rats. Values were presented as mean +/- S.D. for 6 animals in a group. *p<0.05, (*vs* control), ♦p<0.05 (*vs* control pellets)

In the group treated with sterile cotton pellets, a statistically significant increase of phagocytic capacity of peripheral blood PMN (*p<0.05) and a decrease in the serum complement activity (*p<0.05), compared to the rats without granuloma was noted after 24 hours, as well as after 7 days. These changes were in agreement with the literature communicated data, being explained by the immune modifications induced after the development of the local subacute inflammatory reaction [66].

The subcutaneous administration of pellets impregnated with DCF was accompanied by a considerable (♦$p<0.05$) diminution in the phagocytic capacity of peripheral blood PMN, compared to the control group with pellets after 24 hours and 7 days in the experiment.

In the groups 4, 5, 6, 7 an important reduction in the phagocytic capacity of peripheral blood PMN was observed, at 7 days after the samples' administration. There were no important variations in the activity of serum complement between groups 3, 4, 5, 6,7 and the control group without implant during the experiment.

Therefore, by analyzing all these data it can be concluded that the used matrices for the DCF drug do not induce a supplementary toxicity than the drug itself on rats. Moreover, by comparing the samples one to each other, it can be observed that there are no significant differences in terms of their effect on the blood and liver parameters, all of them being safely to be used for bio-applications.

3.9 Evaluation of the nociceptive reactivity

The evaluation of the nociceptive reactivity was evaluated by the tail flick assay which consists in the evaluation of the tail withdrawal latencies in rats, after the administration of analgesic drugs. Besides the fact that DCF is a well-known anti-inflammatory drug, its analgesic effect was also demonstrated, being largely used in the treatment of acute or chronic pain and inflammation and also used as a reference when new analgesics are evaluated [67, 68].

The implantation of the sterile cotton pellets (**Cp**) was associated with a slight diminution of the tail withdrawal latency, suggesting a tendency for hyperalgesic reactivity, but statistically non-significant compared to control group without pellets (**C**).

The treatment with pellets impregnated with DCF determined a rapidly and statistically significant (**$p<0.01$) increase of the latency response, effect prolonged 3 hours (**$p<0.01$) after the subcutaneous implantation, and an abruptly decrease thereafter.

The subcutaneous administration of the hydrogels pellets was accompanied by a substantial increase in the latency time reactivity, beginning 1 day (**$p<0.01$) after the implantation and running for around 3 days (**$p<0.01$) in tail flick test in rats. The most intense effects were noted in animals from group 6 (**H1.5D**). The influence of the tested formulations on the somatic nociceptive sensitivity was in the descending order the following: **DCF > H1.5D > H1.5*D > S1D > S2D**.

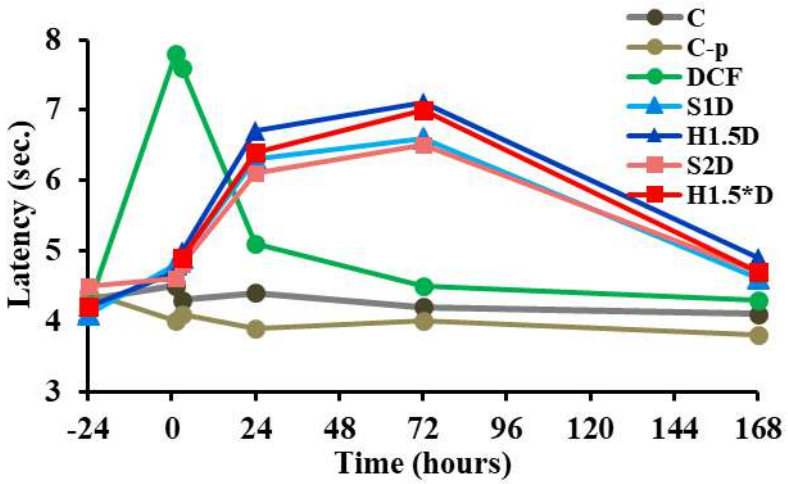

Figure 11. The tail withdrawal latency as a response to thermal noxious stimulation in tail flick test in rats. Each point is the mean ± S.D. of latency time (seconds) for six animals in a group. ** p< 0.01 *vs* control.

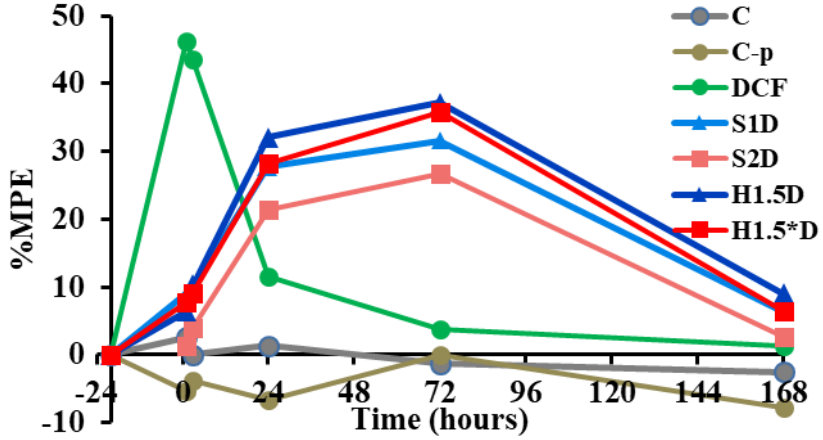

Figure 12. Time course of the maximum possible effect (%MPE) of implanted pellets in tail flick test in rats. Each point is the mean ± S.D. of percentage of maximum possible effect (%MPE) for six animals in a group.

The treatment with pellets impregnated with DCF determined an increase in %MPE in the tail flick test, statistically significant in the first 3 hours, with the peak effect detected 1 hour (46.2 %MPE) after their implantation. In the interval between 1 day and 3 days, the use of hydrogels pellets, significantly increased the response latency, the %MPE of group 6 (**H1.5D**) being more accentuated than of the other groups in all moments of determination, after 3 hours in the tail flick assay.

The *in vivo* tests on rats demonstrated that the hydrogels used as DCF delivery systems present the tremendous advantage of being able to produce an *in vivo* sustained release of the active principle, generating a prolonged effect in the tail flick test in rats, up to several days. The PEG-ylated chitosan derivatives used as reference samples, being more hydrophilic, released the anti-inflammatory drug much faster *in vivo*, data which are in agreement with the faster release rate of these samples from the *in vitro* release kinetics.

4. Conclusions

The present paper reports the synthesis of new hydrogels and drug delivery systems based on PEG-ylated chitosan derivatives and citral, as promising materials for local therapy applications. The hydrogels were obtained by the acid condensation reaction of the amino groups of two PEG-ylated chitosan derivatives and the aldehyde groups of citral, while the drug delivery systems were synthesized by an *in situ* hydrogelation procedure of the same PEG-ylated chitosan derivatives, in the presence of the DCF drug.

This synthetic procedure of the drug delivery systems led to xerogels in which the drug was dispersed at submicrometric level into the xerogels pores walls as demonstrated by SEM and POM, being anchored by physical interactions and leading by this to a sustained release of the encapsulated drug. The drug release profile of the samples is characteristic to systems with sustained release, with a burst effect in the first 4 hours, when a shock dose is necessary, followed by a quite large interval in which the therapeutic dose is kept constant (up to 7 days). The *in vivo* release profile, monitored on rats revealed that the understudy materials present antinociceptive effect for more than 3 days, in comparison to the systemic administration for which the therapeutic effect lasted less than 24 hours. The citryl-imine-PEG-ylated chitosan hydrogels were biologically friendly and biodegradable in the presence of lysozyme, an important enzyme found in the human body.

All the evidences from this study point towards the idea that the use of PEG-ylated chitosan derivatives as precursors for the obtaining of hydrogels seems to be a reliable method for the preparation of biocompatible materials, which meet the requirements imposed by bio-applications and with real chances to pass the gap between fundamental to practical research.

Acknowledgements

This work was supported by the Romanian National Authority for Scientific Research MEN – UEFISCDI (grant number PN-III-P1-1.2-PCCDI2017-0569, no. 10PCCDI/2018) and by the project H2020-MSCA-RISE-2019: Smart Wound Monitoring Restorative Dressings (SWORD) (no. 873123).

References

[1] A. Kakkar, G. Traverso, O.C. Farokhzad, R. Weissleder, R. Langer, Evolution of macromolecular complexity in drug delivery systems, Nat. Rev. Chem. 1 (2017) 0063.

[2] G. Tiwari, R. Tiwari, B. Sriwastawa, L. Bhati, S. Pandey, P. Pandey, S.K. Bannerjee, Drug delivery systems: An updated review. Int. J. Pharm. Investig. 2 (2012) 2-11.

[3] J. Jacob, J.T. Haponiuk, S. Thomas, S. Gopi, Biopolymer based nanomaterials in drug delivery systems: A review, Mater Today Chem. 9 (2018) 43-55.
[4] R. Tiwari, Controlled release drug formulation in pharmaceuticals: a study on their application and properties, World J. Pharm. Res. 5 (2016) 1720-1740.
[5] M.R. Prausnitz, R. Langer, Transdermal drug delivery. Nat. Biotechnol. 26 (2008) 1261-1268.
[6] X. Yu, T. Wen, P. Cao, Pei, Alginate-chitosan coated layered double hydroxide nanocomposites for enhanced oral vaccine delivery, J. Colloid Interface Sci., 556 (2019) 258-265
[7] J.F. Jin, L.L. Zhu, M. Chen, H.-M. Xu, H.-F. Wang, X.-Q. Feng, X.-P. Zhu, Q. Zhou, The optimal choice of medication administration route regarding intravenous, intramuscular, and subcutaneous injection. Patient Prefer. Adherence. 9 (2015) 923-942.
[8] D. Sivakumaran, D. Maitland, T. Oszustowicz, Tuning drug release from smart microgel-hydrogel composites via cross-linking, J. Colloid Interface. Sci., 392 (2013) 422-430.
[9] M.-A. Gagnon, M. Lafleur, Comparison of the structure and the transport properties of low-set and high-set curdlan hydrogels, J. Colloid Interface. Sci. 357 (2011) 419-427.
[10] S. Farrukh, K. Mustafa, A. Hussain, M. Ayoub, Synthesis and Applications of Carbohydrate-Based Hydrogels, Cellulose-Based Superabsorbent Hydrogels, Springer International Publishing AG, part of Springer Nature, Md. I. H. Mondal (ed.) (2018).
[11] I.M.E. Sherbiny, H.Y. Magdi, Hydrogel scaffolds for tissue engineering: progress and challenges. Glob. Cardiol. Sci. Pract. 3 (2013) 316-342.
[12] Y. Liang, X. Zhao, P.X. Ma, B. Guo, Y. Du, X. Han, pH-responsive injectable hydrogels with mucosal adhesiveness based on chitosan-grafted-dihydrocaffeic acid and oxidized pullulan for localized drug delivery, J. Colloid Interface Sci. 536 (2019) 224-234.
[13] Qu, J., Zhao, X., Ma, P.X., Guo, B., pH-responsive self-healing injectable hydrogel based on N-carboxyethyl chitosan for hepatocellular carcinoma therapy, Acta Biomat. 58 (2017)168-180.
[14] J. He, M. Shi, Y. Liang, B. Guo, Conductive adhesive self-healing nanocomposite hydrogel wound dressing for photothermal therapy of infected full-thickness skin wounds, Chem. Eng. J. 394 (2020), 124888.
[15] L. Zhang, L. Wang, B. Guo, P.X. Ma, Cytocompatible injectable carboxymethylchitosan/N-isopropylacrylamide hydrogels for localized drug delivery, Carbohydr. Polym. 103 (2014) 110-118.
[16] J. Qu, X. Zhao, Y. Liang, T. Zhang, P.X. Ma, B. Guo, Antibacterial adhesive injectable hydrogels with rapid self-healing, extensibility and compressibility as wound dressing for joints

skin wound healing, Biomaterials 183 (2018) 185-199.
[17] . J. Qu, X. Zhao, P.X. Ma, B. Guo, Injectable antibacterial conductive hydrogels with dual response to an electric field and pH for localized “smart” drug release, Acta Biomat. 72 (2018) 55-69.
[18] X. Yanshuang, L. Yongsan, C. Qiaomei, F. Lihua, T. Lei, W. Yen, Injectable and self-healing chitosan hydrogel based on imine bonds: design and therapeutic applications. Int. J. Mol. Sci. 19 (2018) 2198.
[19] H. Palacio, F. Otalvaro, L. Giraldo, G. Ponchel, F. Segura-Sanchez, Chitosan-acrylic polymeric nanoparticles with dynamic covalent bonds. Synthesis and stimuli behavior. Chem. Pharm. Bull. 65 (2017) 1132-1143.
[20] E. Bakaic, N.M.B. Smeets, T. Hoare, Injectable hydrogels based on poly(ethylene glycol) and derivatives as functional biomaterials, RSC Adv. 5 (2015) 35469-35486.
[21] L. Marin, S. Morariu, M.C. Popescu, A. Nicolescu, C. Zgardan, B.C. Simionescu, M. Barboiu, Out-of-Water constitutional self-organization of chitosan–cinnamaldehyde dynagels. Chem. Eur. J. 20 (2014) 4814-4821.
[22] D. Ailincai, L. Marin, S. Morariu, M. Mares, A.C. Bostanaru, M. Pinteala, B.C. Simionescu, M. Barboiu, Dual crosslinked iminoboronate-chitosan hydrogels with strong antifungal activity against Candida planktonic yeasts and biofilms. Carbohyd. Polym. 152 (2016) 306-316.
[23] A.M. Olaru, L. Marin, S. Morariu, G. Pricope, M. Pinteala, L. Tartau-Mititelu. Biocompatible chitosan based hydrogels for potential application in local tumour therapy. Carbohyd. Polym. 179 (2018) 59-70.
[24] A. Bejan, D. Ailincai, B.C. Simionescu, L. Marin, Chitosan hydrogelation with a phenothiazine based aldehyde: a synthetic approach toward highly luminescent biomaterials. Polym. Chem. 9 (2018) 2359-2369.
[25] M.M. Iftime, S. Morariu, L. Marin, Salicyl-imine-chitosan hydrogels: Supramolecular architecturing as a crosslinking method toward multifunctional hydrogels. Carbohyd. Polym. 165 (2017) 39-50.
[26] L. Marin, D. Ailincai, S. Morariu, L. Tartau-Mititelu, Development of biocompatible glycodynameric hydrogels joining two natural motifs by dynamic constitutional chemistry. Carbohyd. Polym. 170 (2017) 60-71.
[27] K. Knop, R. Hoogenboom, D. Fischer, U.S. Schubert, Poly(ethylene glycol) in drug delivery: pros and cons as well as potential alternatives, Angew. Chem. Int. 49 (2010) 6288-6308.

[28] L. Casettari, D. Vllasaliu, E. Castagnino, S. Stolnik, S. Howdle, L. Illum, PEGylated chitosan derivatives: Synthesis, characterizations and pharmaceutical applications, Progress in Polym. Sci. 37 (2012) 659-685.

[29] E. Lih, J.S. Lee, K.M. Park, K.D. Park, Rapidly curable chitosan–PEG hydrogels as tissue adhesives for hemostasis and wound healing, Acta Biomater. 8 (2012) 3261-3269.

[30] G. Jiang, J. Sun, F. Ding, PEG-g-chitosan thermosensitive hydrogel for implant drug delivery: cytotoxicity, in vivo degradation and drug release, J. Biomater. Sci. Polym. Ed. 25 (2014) 241-256.

[31] C.-T. Tsao, F.M. Kievit, A. Ravanpay, A.E. Erickson, M.C. Jensen, R.G. Ellenbogen, M. Zhang, Thermoreversible Poly(ethylene glycol)-g-Chitosan Hydrogel as a Therapeutic T Lymphocyte Depot for Localized Glioblastoma Immunotherapy, Biomacromolecules. 15 (2014) 2656-2662.

[32] C.B. Silva, S.S. Guterres, V. Weisheimer, E.E. Schapoval, Antifungal activity of the lemongrass oil and citral against Candida spp., Braz. J. Infect. Dis. 12 (2008) 63-66.

[33] SIDS, SIDSinitialassessmentfor13thSIAM,CitralCASNo.5392-40-5, 2001.

[34] O.I. Afanasyev, E. Kuchuk, D.L. Usanov, D. Chusov, Reductive amination, Chem. Rev. 119 (2019) 11857-11911.

[35] D. Ailincai, L. Tartau-Mititelu, L. Marin, Drug delivery systems based on biocompatible imino-chitosan hydrogels for local anticancer therapy. Drug deliv. 25 (2018) 1080-1090.

[36] A. M. Craciun, L. Mititelu Tartau, M. Pinteala, L. Marin, Nitrosalicyl-imine-chitosan hydrogels based drug delivery systems for long term sustained release in local therapy, J. Colloid Interface Sci. 15 (2019) 196-207.

[37] C.-A. Ghiorghita, F. Bucatariu, E.S. Dragan, Sorption/release of diclofenac sodium in/from free-standing poly(acrylic acid)/poly(ethyleneimine) multilayer films, J. Appl. Polym. Sci. 133 (2016) 31.

[38] R. Chandrawati, Enzyme-responsive polymer hydrogels for therapeutic delivery. Exp. Biol. Med. 241 (2016) 972-979.

[39] J.S. Mogil, Animal models of pain: progress and challenges, Nat. Rev. Neurosci. 10 (2009) 283-294.

[40] R. Rand, A. Burton, T. Ing. The tail of the rat, in temperature regulation and acclimatization. NRC Research Test. (2012) 257-267.

[41] D. Le Bars, M. Gozariu, S. Cadden, Animal Models of Nociception. J. Pharmacol. Exp. Ther. 53 (2001) 597-652.

[42] C. Ma, Animal models of pain, Int. Anesthesiol. Clin. 45 (2007) 121-131.

[43] I.L. Torres, A.P. Vasconcellos, S.N. Silveira Cucco, C. Dalmaz, Effect of repeated stress on novelty-induced antinociception in rats. Braz. J. Med. Biol. Res. 34 (2001) 241-244.
[44] M.F. Wolf, J.M. Andwraon, Practical approach to blood compatibility assessments: general considerations and standards, Biocompatibility and Performance of Medical Devices, Woodhead Publishing (2012).
[45] M. Peacman, Clinical & Experimental Immunology, British Society of Immunology, Wiley Library (2011).
[46] E.J. Peacock, Th. Rusell, D. Thomas, Manual of Laboratory Immunology, Lea and Febiger Publisher, Philadelphia (1980).
[47] C. Carvalho, A. Gaspar, A. Knight A, L. Vicente. Ethical and scientific pitfalls concerning laboratory research with non-human primates, and possible solutions. Animals. 29 (2018) 9.
[48] *** Directive 2010/63/EU of the European Parliament and of the Council of 22 September 2010 on the protection of animals used for scientific purposes.
[49] M. Zimmerman, Ethical guidelines for investigations of experimental pain in conscious animals, Pain. 16 (1983) 109-110.
[50] L. Marin, B. Simionescu, M. Barboiu, Imino-chitosan biodynamers, Chem. Comm. 48 (2012) 8778-8780.
[51] F.-J. Li, S.-D. Zhang, J.-Z. Liang, J.-Z. Wang, Effect of polyethylene glycol on the crystallization and impact properties of polylactide-based blends, Polym. Adv. Technol. 26 (2005) 465-475.
[52] I. Leceta, P. Guerrero, I. Ibarburu, M.T. Duenas, K. De la Caba, Characterization and antimicrobial analysis of chitosan-based films, J. Food Eng. 116 (2013) 889-899.
[53] L. Marin, S. Destri, W. Porzio, F. Bertini, Synthesis and characterization of new azomethine derivatives exhibiting liquid crystalline properties. Liq. Cryst. 36 (2009) 21-32.
[54] A. Zabulica, E. Perju, M. Bruma, L. Marin, Novel luminescent liquid crystalline polyazomethines. Synthesis and study of thermotropic and photoluminescent properties. Liq. Cryst. 41 (2014) 252-262.
[55] F.J. Deng, H.J. Zhou, J.Y. Chen, H.Y. Huang, J.W. Tian, Y.Q. Wen, Q. Huang, M.Y. Liu, X.Y. Zhang, Y. Wei, Surface PEGylation and biological imaging of fluorescent Tb3+-doped layered double hydroxides through the photoinduced RAFT polymerization, J. Colloid Interface Sci. 532 (2018) 641-649.
[56] C.N. Schnell, M.V. Galvan, M.A. Zanuttini, P. Mocchiutti, Hydrogels from xylan/chitosan complexes for the controlled release of diclofenac sodium, Cellulose. 27 (2020) 1465-1481.

[57] X. Qi, X. Qin, R. Yang, J. Qin, W. Li, K. Luan, Z. Wu, L Song, Intra-articular administration of chitosan thermosensitive *in situ* hydrogels combined with diclofenac sodium loaded alginate microspheres, J. Pharm. Sci. 105 (2016) 122-130.
[58] U.G. Spizzirri, F. Iemma, G. Cirillo, I. Altimari, F. Puoci, N. Picci, Temperature-sensitive hydrogels by graft polymerization of chitosan and N-isopropylacrylamide for drug release, Pharm. Dev. Tech. 18 (2013) 1026-1034.
[59] Q. Wang, J. Zhang, A. Wang, Preparation and characterization of a novel pH-sensitive chitosan-g-poly (acrylic acid)/attapulgite/sodium alginate composite hydrogel bead for controlled release of diclofenac sodium, Carbohydr. Polym. 78 (2009) 731-737.
[60] N. Benkerroum, Antimicrobial activity of lysozyme with special relevance to milk, Afr. J. Biotechnol. 7 (2008) 4856-4867.
[61] N.A. Peppas, B. Narasimhan, Mathematical models in drug delivery: How modeling has shaped the way we design new drug delivery systems, J. Control. Release. 190 (2014) 75-81.
[62] M. Bruschi, Strategies to Modify the Drug Release from Pharmaceutical Systems, Woodhead Publishing, (2015).
[63] G. Singhvi, M. Singh, Review: in-vitro drug release characterization models, Int. J. Pharm. Sci. Rev. Res. 2 (2011) 77-84.
[64] I.O. de Solorzano, T. Alejo, M. Abad, C. Bueno-Alejo, G. Mendoza, V. Andreu, S. Irusta, V. Sebastian, M. Arruebo, Cleavable and thermo-responsive hybrid nanoparticles for on-demand drug delivery, J. Colloid Interface Sci. 533 (2019) 171-181.
[65] S. Hirano, Y. Yagi, The effects of N-substitution of chitosan and the physical form of the products on the rate of hydrolysis by chitinase from streptomyces griseus, Carbohydr. Res. 83 (1980) 103-108.
[66] C.E. Lupuşoru Imunofarmacologie, Ed Alfa, Iaşi (2001) 33-89, 198-202, 248-251.
[67] T. Kantor, Use of Diclofenac in Analgesia, The American Journal of Medicine. 80 (1986) 64-69.
[68] M. Moniruzzaman, M.Z. Imam, Evaluation of antinociceptive effect of methanolic extract of leaves of Crataeva nurvala Buch.-Ham. BMC Complement. Altern. Med. 14 (2014) 354-361.